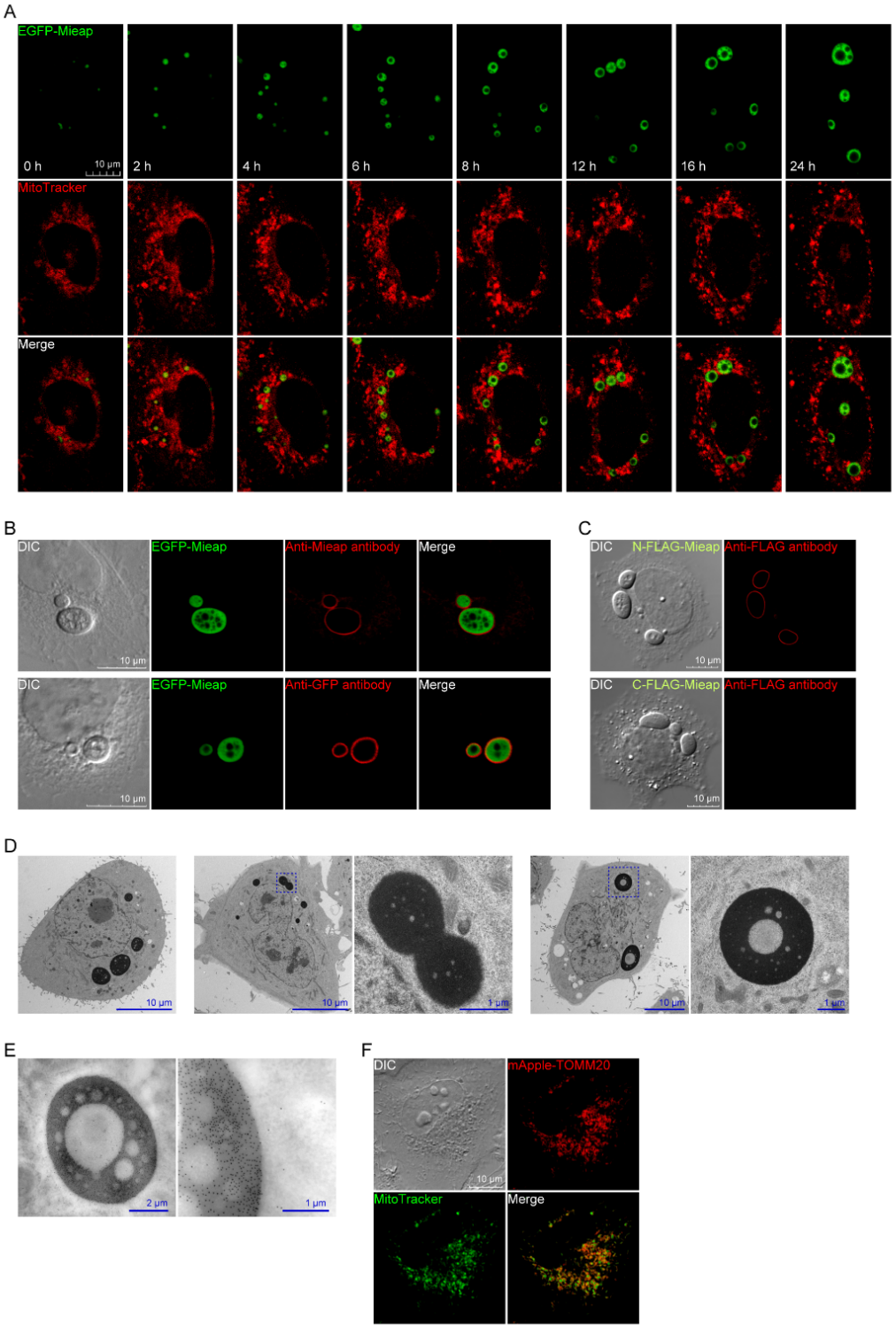

Fig. S1. Mieap forms liquid droplets.

(A) Time-lapse imaging of a cell expressing EGFP-Mieap. A549-cont cells were infected with Ad-EGFP-Mieap. Image acquisition was started 10.5 h after infection of Ad-EGFP-Mieap, and 0.5 h after MitoTracker Red treatment. See also Video S1.

(B) Comparative imaging of EGFP-Mieap condensates, visualized with both EGFP-Mieap and immunofluorescence (IF) using anti-Mieap antibody (upper panel) or anti-GFP antibody (lower panel) in A549 cells.
(C) IF imaging of N-FLAG-Mieap condensates (upper panel) or C-FLAG-Mieap condentates (lower panel) using anti-FLAG antibody in A549 cells.
(D) Transmission electron microscopy of Mieap condensates stained with osmium (OsO_4). A549-cont cells (left) and U373MG cells (middle and right) are shown.
(E) Post-embedding immunoelectron microscopy of Mieap condensates using anti-Mieap antibody.
(F) Live-cell imaging to verify subcellular localization of mApple-TOMM20. A549-cont cells were infected with Ad-mApple-TOMM20 and subsequently treated with MitoTracker Green.

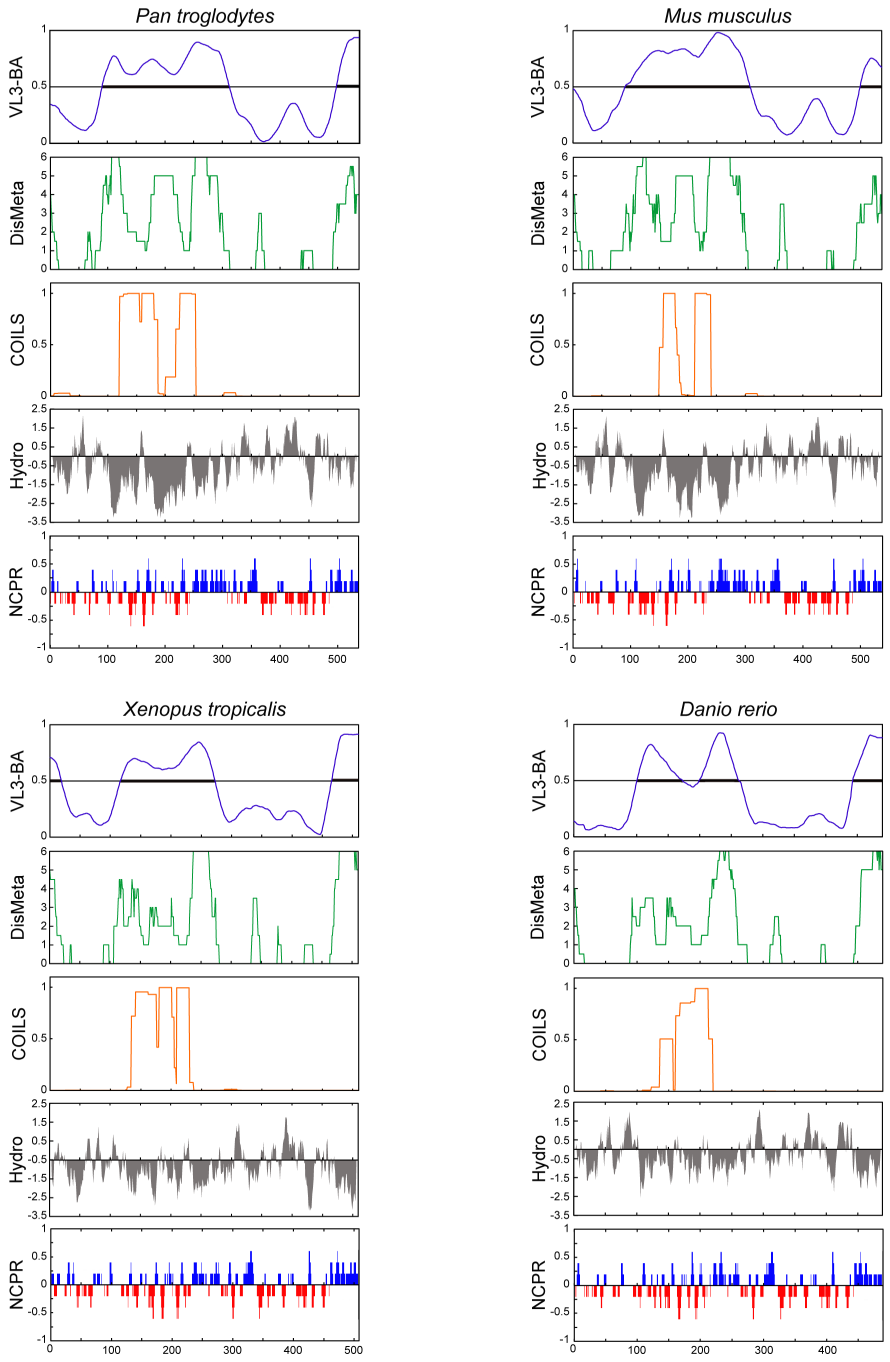

Fig. S2. Analyses of Mieap orthologs.

Amino acid sequence analyses of representative Mieap orthologs, as in Figure 2E.

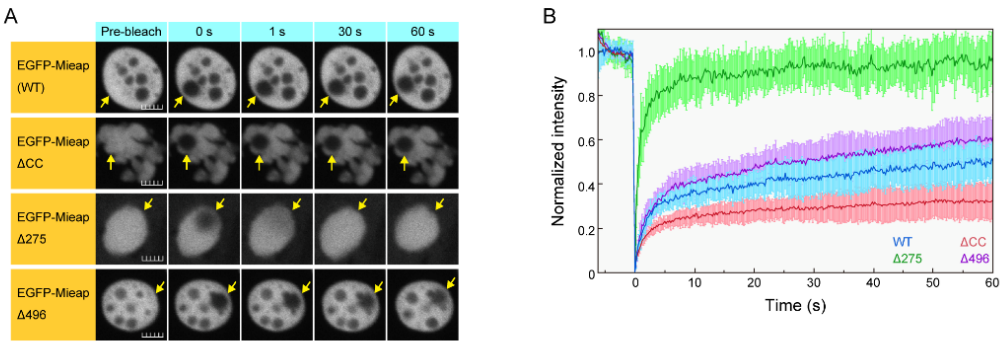

Fig. S3. FRAP analysis of condensates formed by EGFP-Mieap and three deletion mutants.
(A) Representative FRAP images of condensates formed by EGFP-Mieap (WT) and three deletion mutants (ΔCC, Δ275, and Δ496) in A549-cont cells. Each condensate was subjected to spot-bleach using a 488-nm laser at 10% laser power with 11.6 μs/μm exposure time and followed up for 60 s. Bleached areas are indicated by yellow arrows. Scale bar, 2 μm.
(B) Plotting of normalized average fluorescence recovery in the FRAP experiment with weaker laser exposure. Laser power was weakened to 1.4% and the exposure time was shortened to 1.4 μs/μm. n = 15 condensates for each construct. Data shown are means ±SD.

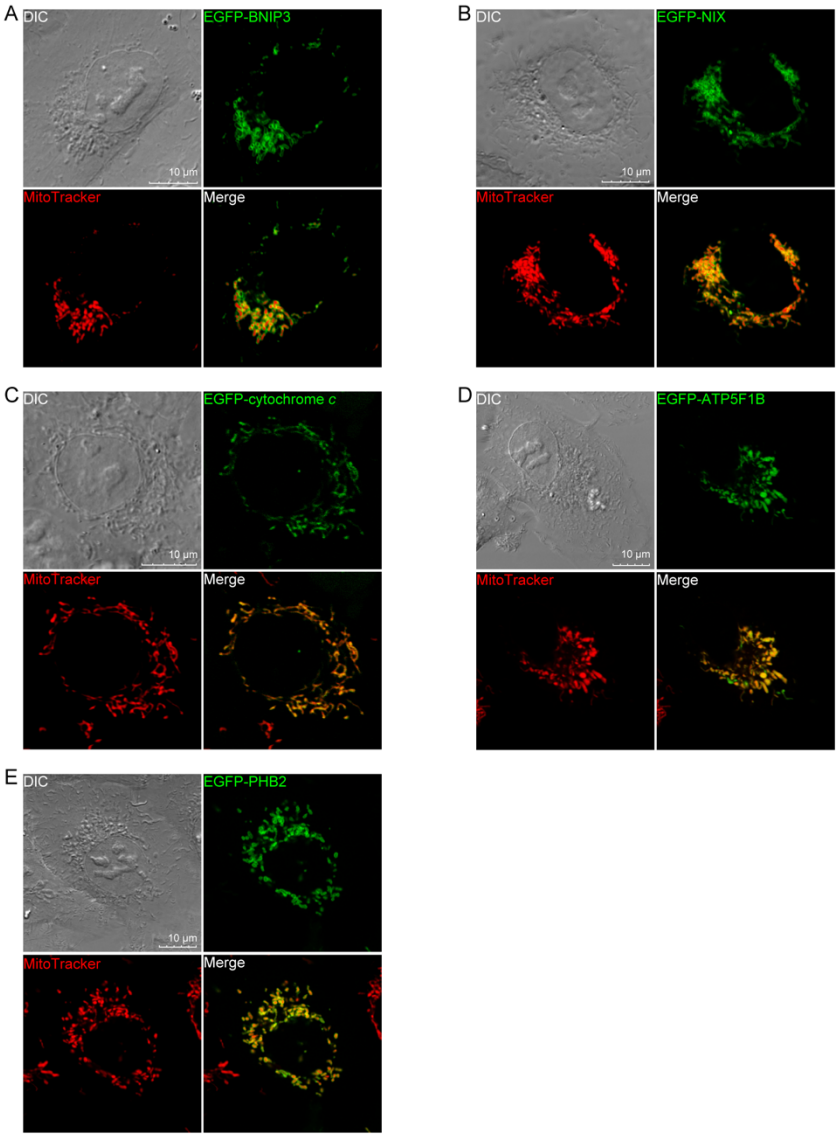

Fig. S4. Verification of subcellular localization of fluorescently labeled proteins.
(A-E) Subcellular localization of (A) EGFP-BNIP3, (B) EGFP-NIX, (C) EGFP-cytochrome *c*, (D) EGFP-ATP5F1B, and (E) EGFP-PHB2 verified by confocal live cell imaging, compared with localization of MitoTracker Green or MitoTracker Red in A549 cells.

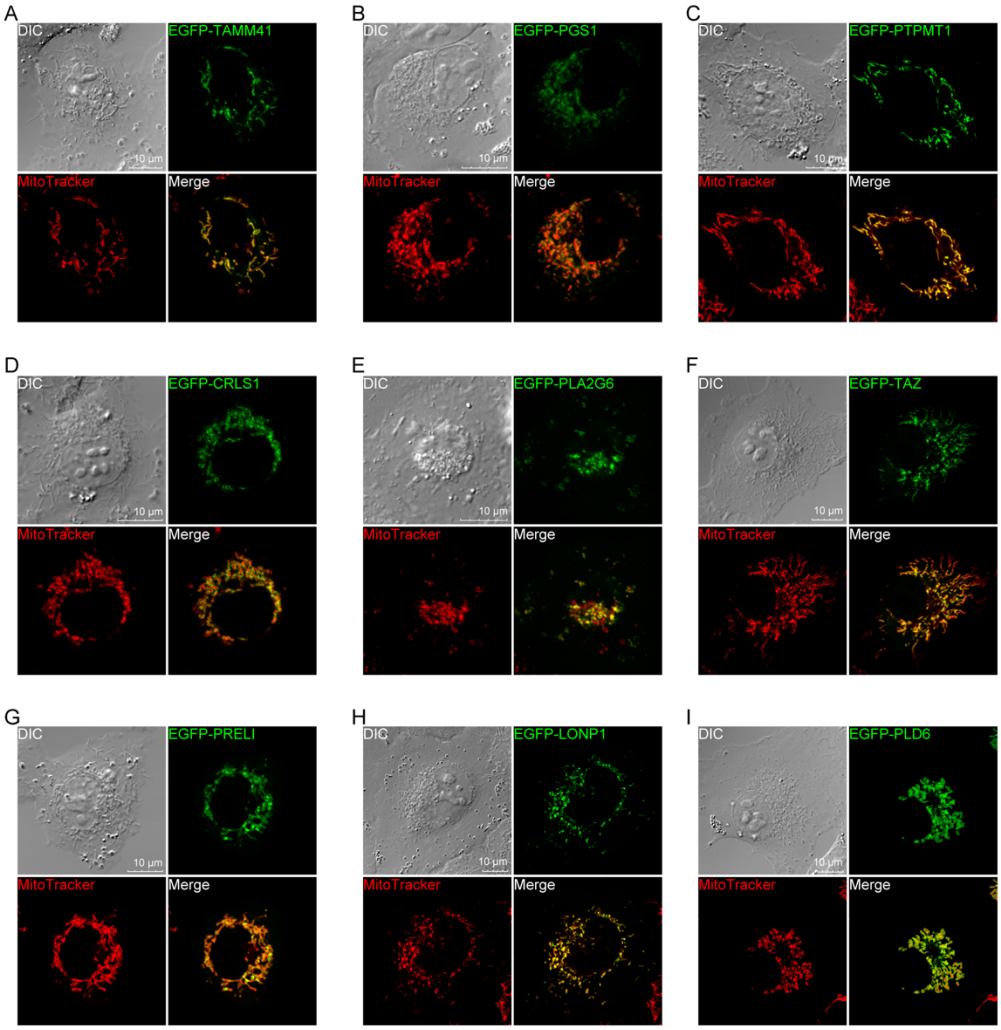

Fig. S5. Verification of subcellular localization of fluorescently labeled proteins.
(A-I) Subcellular localization of (A) EGFP-TAMM41, (B) EGFP-PGS1, (C) EGFP-PTPMT1, (D) EGFP-CRLS1, (E) EGFP-PLA2G6, (F) EGFP-TAZ, (G) EGFP-PRELI, (H) EGFP-LONP1, and (I) EGFP-PLD6 verified by confocal live cell imaging, compared with localization of MitoTracker Red in A549 cells.

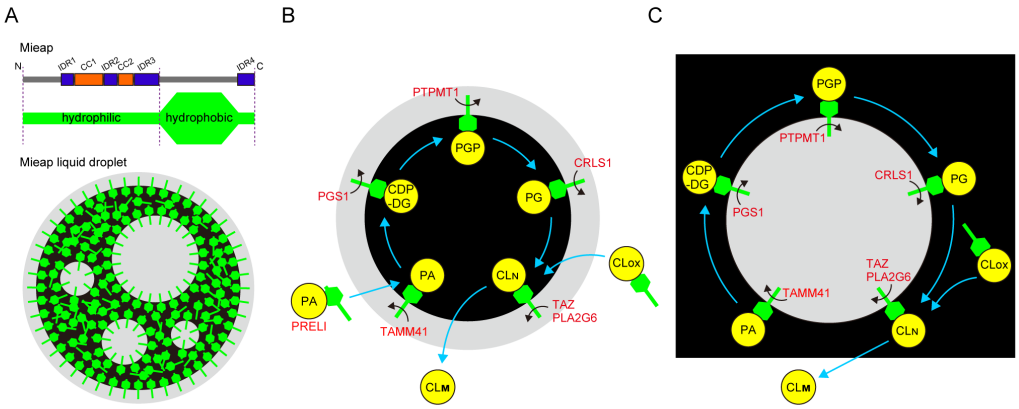

Fig. S6. Hypothetical models for biosurfactant activity of Mieap and Mieap-mediated sequential enzymatic reactions in CL metabolism.

(A) Hypothetical model of biosurfactant activity of Mieap. Mieap (colored in green) exists in the electron-dense major phase (lipid phase) (in black), as a "scaffold" protein and/or as a potential "biosurfactant." At the boundary between the outside of the Mi-LDs (aqueous phase) and the electron-dense major phase (lipid phase) or between the electron-dense major phase (lipid phase) and electron-lucent minor phase (aqueous phase), the hydrophilic N-terminal end of Mieap always faces aqueous the phase at the boundary.

(B, C) Hypothetical model for Mieap-mediated sequential enzymatic reactions in CL metabolism. Black areas indicate the lipid phase containing CL and Mieap. Gray areas indicate the aqueous phase containing enzymes. Sequential reactions occur at the interface between the outside of the Mi-LDs (aqueous phase) and the major phase (lipid phase) (B) or between the major phase (lipid phase) and the minor phases (aqueous phase) (C). Once Mieap (green) stably interacts with PA via its C-terminal region, one of the enzymes transiently and weakly interacts with the N-terminal region of Mieap. When Mieap interacts with TAMM41, PA is converted to CDP-DG. Such reactions between biosynthetic enzymes and corresponding substrates could be repeated until mature CL is produced. Molecular crowding of enzymes and substrates at the surfaces of Mi-LDs, phase separation of enzymes and substrates, multivalent interaction of Mieap with enzymes, and the biosurfactant activity of Mieap may enable efficient sequential reactions for CL metabolism.

Abbreviations: PA, phosphatidic acid; CDP-DG: cytidine diphosphate diacylglycerol; PGP, phosphatidylglycerophosphate; PG, phosphatidylglycerol; CLOX, oxidized cardiolipin; CLN, nascent cardiolipin; CLM, mature cardiolipin.